Scheme I

$$\left.\begin{array}{c} EH^+ \\ (\text{fast})\ \uparrow\downarrow \pm H^+ \\ E \end{array}\right\} \underset{k_2}{\overset{k_1}{\rightleftharpoons}} \left\{\begin{array}{c} E'H^+ \\ \pm H^+\ \uparrow\downarrow\ (\text{fast}) \\ E' \end{array}\right.$$

at ~325 nm ($\Delta A = -0.012$) and at ~425 nm ($\Delta A = -0.012$) and growth at ~360 nm ($\Delta A = +0.036$) with a rate constant of 0.062 ± 0.002 s^{-1}. No further changes in the spectrum were seen over a time span of several minutes.

The K^+-jump experiment also showed slow conversion of the 420-nm peak to the 340-nm absorption, but the kinetics are not cleanly first order. An approximate first-order rate constant of 0.3–0.5 s^{-1} can be obtained from the data at short times, but the analysis is complicated by continuing changes in absorbance.

Scheme I, or a modified version to include the effects of Na^+-K^+ exchange, accounts for the major observed spectral changes. However, other changes also occur which will require additions to this simple phenomenological scheme. Full analysis of these data including the use of principal component techniques[14] is underway and should further our understanding of the mechanism of tryptophanase catalysis.

References and Notes

(1) This work was supported by National Science Foundation Grant No. PCM 76-18905.
(2) F. C. Happold and A. Struyvenberg, *Biochem. J.*, **58**, 379 (1954).
(3) W. A. Newton and E. E. Snell, *Proc. Natl. Acad. Sci. U.S.A.*, **52**, 382 (1964).
(4) Y. Morino and E. E. Snell, *J. Biol. Chem.*, **247**, 2800 (1967).
(5) C. H. Suelter and E. E. Snell, *J. Biol. Chem.*, **252**, 1852 (1976).
(6) T. Muro, H. Nakatani, K. Hiromi, H. Kumagai, and H. Yamada, *J. Biochem.*, **84**, 633 (1978).
(7) R. J. Ulevitch and R. G. Kallen, *Biochemistry*, **16**, 5350 (1977).
(8) D. S. June and J. Ceraso, manuscript in preparation.
(9) C. H. Suelter, J. Wang, and E. E. Snell, *Anal. Biochem.*, **76**, 221 (1976).
(10) Tryptophanase had a specific activity of 55 μmol min^{-1} mg^{-1} at 30 °C in 0.6 mM *S-o*-nitrophenyl-L-cysteine, 50 mM KCl, and 50 mM potassium phosphate, pH 8.0, according to C. H. Suelter, J. Wang, and E. E. Snell, *FEBS Lett.*, **66**, 230 (1976).
(11) Experiment A: tryptophanase (2.04 mg ml^{-1}) in 1 mM *N,N*-bis(2-hydroxyethyl)glycine, pH 8.53, 0.2 M KCl, 15 μM pyridoxal-P, 1 mM EDTA, and 0.2 mM dithiothreitol was pushed against 50 mM 2(*N*-morpholino)ethane sulfonate, pH 6.72, 0.2 M KCl, 1 mM EDTA, and 15 μM pyridoxal-P. Experiment B: tryptophanase (2.06 mg ml^{-1}) in 1 mM *N*-tris(hydroxymethyl)methyl-2-aminoethane sulfonate, pH 7.38, 0.2 M KCl, 15 μM pyridoxal-P, 1 mM EDTA and 0.2 mM dithiothreitol was pushed against 50 mM 2-(*N*-cyclohexylamino)ethane sulfonate, pH 9.30, 0.2 M KCl, 1 mM EDTA, and 15 μM pyridoxal-P. Experiment C: tryptophanase (2.4 mg ml^{-1}) in 50 mM *N*-2-hydroxyethylpiperazine propanesulfonate, pH 8.0, in 1 mM EDTA, 0.2 mM dithiothreitol, 100 mM NaCl, and 80 μM pyridoxal-P was pushed against 50 mM *N*-2-hydroxyethylpiperazine sulfonate, 1 mM EDTA, 0.2 mM dithiothreitol, and 100 mM KCl.
(12) R. B. Coolen, N. Papadakis, J. Avery, C. G. Enke, and J. L. Dye, *Anal. Chem.*, **47**, 1649 (1975): N. Papadakis, R. B. Coolen, and J. L. Dye, *ibid.*, **47**, 1644 (1975): C. H. Suelter, R. B. Coolen, N. Papadakis, and J. L. Dye, *Anal. Biochem.*, **69**, 155 (1975).
(13) R. J. Johnson and D. F. Metzler, *Methods Enzymol.* **18**, (A), 433 (1970).
(14) R. N. Cochran and F. H. Horne, *Anal. Chem.*, **49**, 846 (1977).
(15) Department of Chemistry.

David S. June, Barbara Kennedy, T. H. Pierce
Sami V. Elias, Folim Halaka, Iraj Behbahani-Nejad
Ashraf El Bayoumi, Clarence H. Suelter, James L. Dye*[15]

Departments of Chemistry, Biophysics, and Biochemistry
Michigan State University, East Lansing, Michigan 48824

Received January 16, 1979

Resonance Raman Studies on Pyrocatechase

Sir:

The intradiol dioxygenases, pyrocatechase and protocatechuate 3,4-dioxygenase, catalyze the cleavage of catechols to yield *cis,cis*-muconic acids.[1] These enzymes contain high-spin ferric iron in the active site and are characterized by a broad absorption band centered near 450 nm (ϵ_M ~3000/Fe). Upon substrate binding, the absorption maximum shifts to the red, accompanied by a significant increase in absorbance in the region above 600 nm.[2,3] Recently, resonance Raman experiments on protocatechuate 3,4-dioxygenase from *Pseudomonas aeruginosa* have shown the presence of tyrosine in the iron coordination site.[4-6] Furthermore, Felton et al.,[6] using 514.5-nm excitation, observed the appearance of new Raman peaks in the spectra of enzyme-substrate and enzyme-inhibitor complexes which were assignable to the respective ligating species, while retaining the tyrosine peaks observed in the native enzyme. They concluded that tyrosine ligation was not altered upon substrate or inhibitor binding.

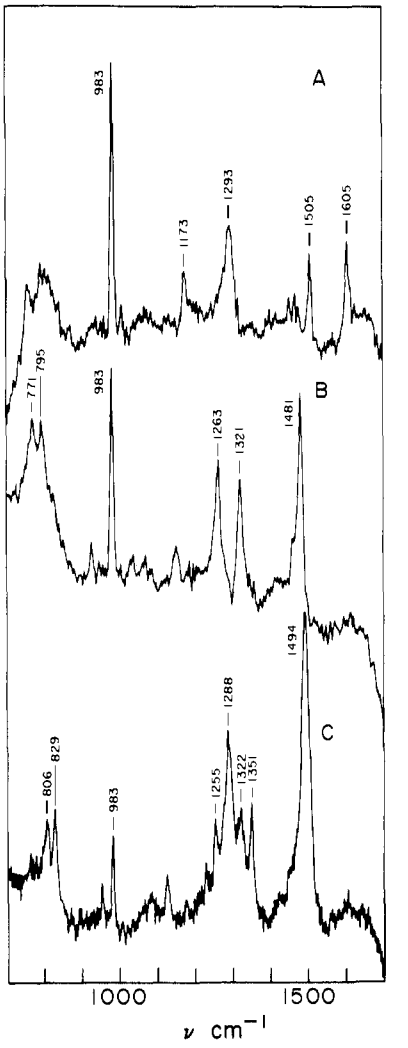

Figure 1. Raman spectra of (A) pyrocatechase; (B) the enzyme-catechol complex, prepared anaerobically, [catechol] = 10 mM; and (C) the enzyme-4-nitrocatechol complex, [4-nitrocatechol] = 0.5 mM. Spectra were obtained using 647.1-nm excitation from a Coherent Radiation Model 500K krypton ion laser and recorded on a Spex 1401 spectrometer interfaced to an Interdata 70 computer. Conditions: 100–150-mW power, 4-cm^{-1} slit width, 20–25 mg/mL of protein in Tris-OAc pH 8.5 buffer, 4 °C sample temperature. SO_4^{2-} was used as internal standard.

We report here the resonance Raman spectra of pyrocatechase from *Pseudomonas arvilla* C-1 and its complexes with catechol and 4-nitrocatechol. The enzyme was prepared according to the procedure of Fujiwara et al.[7] Spectra were obtained using the 647.1-nm line of a krypton laser; this wavelength was selected because of fluorescence problems at shorter wavelengths. Figure 1A shows the Raman spectrum of the native enzyme with peaks at 1173, 1293, 1505, and 1605 cm^{-1}. These vibrations are assigned to tyrosine, analogous to those observed for protocatechuate 3,4-dioxygenase[4,5] and the transferrins.[8,9] Pyrocatechase, thus, joins the list of iron proteins having tyrosine coordination.

0002-7863/79/1501-2219$01.00/0

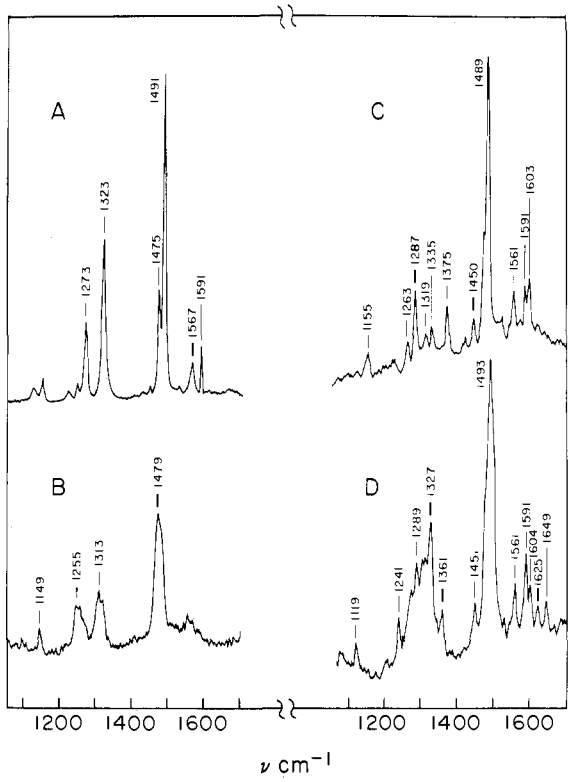

Figure 2. Raman spectra of (A) $[Fe(cat)_3]^{3-}$, (B) $[Fe_2(cat)_4OAc]^{3-}$, (C) Fe(salen)catH, and (D) Fe(salen)ncatH were obtained on 10% KBr pellets at room temperature under instrumental conditions similar to those given for Figure 1.

Upon addition of catechol, new Raman peaks at 1263, 1321, and 1481 cm^{-2} are observed (Figure 1B); the tyrosine peaks, however, have disappeared. Although this may indicate the displacement of tyrosine by the substrate, we suggest an alternative explanation. Spectra obtained on the protocatechuate 3,4-dioxygenase-3-(3′,4′-dihydroxyphenyl)propionate complex using 647.1-nm excitation show peaks due only to the substrate (at 1269, 1319, and 1471 cm^{-1}), in accord with our results. This is in contrast to the spectrum reported by Felton et al.[6] using 514.5-nm excitation. We suggest that the visible spectrum of the enzyme-substrate complexes of these two dioxygenases consists of the superposition of at least two charge-transfer interactions—the iron-tyrosine interaction as observed in the native enzymes and the iron-catechol interaction which is manifested by the increase in absorbance in the longer wavelength region upon substrate binding. The iron-tyrosine charge-transfer band is apparently blue shifted in the enzyme-substrate complex, to the extent that this band is no longer in resonance with the 647.1 nm exciting wavelength. This would account for the disappearance of the tyrosine vibrations in the enzyme-substrate complex. An excitation profile study of one such complex would clearly be very useful to fully understand the visible spectra of these complexes.

The Raman spectrum of the 4-nitrocatechol complex (Figure 1C) is also markedly different from that of the native enzyme. 4-Nitrocatechol is a good competitive inhibitor for pyrocatechase and spectral changes similar to those with catechol are observed upon binding.[10] The most striking feature of the Raman spectrum of the 4-nitrocatechol complex is the peak at 1494 cm^{-1}. This is not observed in solutions of the neutral nitrocatechol, its monoanion, or its dianion.[11]

In order to elucidate the nature of substrate interaction with enzyme, several iron-catechol complexes[12] were synthesized and their Raman spectra were compared. $[Fe(cat)_3]^{3-}$ [13] and $[Fe_2(cat)_4OAc]^{3-}$ [14] have been reported. Fe(salen)catH and Fe(salen)ncatH were synthesized by ligand exchange reactions of Fe(salen)OAc[15] in CH_2Cl_2 with an excess of the desired catechol. Fe(salen)catH[16] was recrystallized in acetonitrile-ethyl acetate yielding purple needles. Calcd for $C_{22}H_{19}FeN_2O_4$: C, 61.27; H, 4.48; Fe, 12.95; N, 6.50. Found: C, 61.59; H, 4.46; Fe, 12.94; N, 6.63. We suggest a structure wherein the catechol occupies an axial position, coordinating through only one hydroxyl group. The presence of the remaining O-H bond is indicated by the shift of ν_{OH} from 3380 to 2520 cm^{-1} observed when catechol deuterated at the hydroxyl groups was used for the synthesis of the complex.

The Raman spectra of these complexes are shown in Figure 2. The spectrum of $[Fe(cat)_3]^{3-}$ (Figure 2A) is similar to the one reported by Salama et al.,[17] though the peak intensities are somewhat different owing to the 647.1-nm exciting wavelength. The peaks observed for $[Fe_2(cat)_4OAc]^{3-}$ (Figure 2B) correspond to those in $[Fe(cat)_3]^{3-}$ but are broader, suggesting that the technique is sensitive to the two modes of catechol coordination in this complex. The spectrum of Fe(salen)catH (Figure 2C) exhibits peaks due to both salen and catechol ligands. A comparison with the spectrum of Fe(salen)OAc shows that three peaks in the 1200-1600-cm^{-1} region arise from catechol—1287, 1375, and 1489 cm^{-1}. The three catechol complexes exhibit a peak near 1485 cm^{-1}, which appears to be characteristic of the catechol-iron interaction. This has been assigned to the stretching of the carbon-carbon bond to which the oxygens are attached.[17] The region around 1300 cm^{-1} appears to be indicative of the ionization state of the catechol. Where both of the catechol protons are off, as in $[Fe(cat)_3]^{3-}$ and $[Fe_2(cat)_4(OAc)]^{3-}$, peaks near 1260 and 1320 cm^{-1} are observed, whereas peaks at 1287 and 1375 cm^{-1} are observed for Fe(salen)catH.

The spectrum of Fe(salen)ncatH (Figure 2D) exhibits features similar to the other catechol complexes, especially the 1493-cm^{-1} peak indicating iron coordination and closely resembles that of the enzyme-4-nitrocatechol complex. On the other hand, the Raman spectrum of the enzyme-catechol complex clearly matches the spectra of the chelated, dianionic catecholates more closely than that of the monoanionic Fe(salen)catH. These spectra suggest that catechol indeed binds to the active site iron and that catechol loses both its protons upon binding. They further suggest that catechol may be chelated to the iron in the active site. Further experiments are in progress to elucidate the nature of the enzyme-substrate interaction.

Acknowledgments. This research was supported by the Research Corporation and the National Institutes of Health (GM 25422). We thank S. L. Han and K. B. C. Goh for experimental assistance.

References and Notes

(1) Nozaki, M. In "Molecular Mechanisms of Oxygen Activation", Hayaishi, O., Ed.; Academic Press: New York, 1970; Chapter 4.
(2) Kojima, Y.; Fujisawa, H.; Nakazawa, A.; Nakazawa, T.; Kanetsuna, F.; Taniuchi, H.; Nozaki, M.; Hayaishi, O. *J. Biol. Chem.* **1967**, *242*, 3270–3278.
(3) Fujisawa, H.; Uyeda, M.; Kojima, Y.; Nozaki, M.; Hayaishi, O. *J. Biol. Chem.* **1972**, *247*, 4414–4421.
(4) Tatsuno, Y.; Saeki, Y.; Iwaki, M.; Yagi, T.; Nozaki, M.; Kitagawa, T.; Otsuka, S. *J. Am. Chem. Soc.* **1978**, *100*, 4614–4615.
(5) Keyes, W. E.; Loehr, T. M.; Taylor, M. L. *Biochem. Biophys. Res. Commun.* **1978**, *83*, 941–945.
(6) Felton, R. H.; Cheung, L. D.; Phillips, R. S.; May, S. W. *Biochem. Biophys. Res. Commun.* **1978**, *85*, 844–850.
(7) Fujiwara, M.; Golovleva, L. A.; Saeki, Y.; Nozaki, M.; Hayaishi, O. *J. Biol. Chem.* **1975**, *250*, 4848–4855.
(8) Tomimatsu, Y.; Kint, S.; Scherer, J. R. *Biochemistry* **1976**, *15*, 4918–4924.
(9) Gaber, B. P.; Miskowski, V.; Spiro, T. G. *J. Am. Chem. Soc.* **1974**, *96*, 6868–6873.
(10) Tyson, C. A. *J. Biol. Chem.* **1975**, *250*, 1765–1770.
(11) In contrast, Raman spectra of protocatechuate 3,4-dioxygenase with 4-nitrocatechol exhibit peaks due to the native enzyme and the nitrocatechol dianion, in agreement with the visible spectrum of the complex.[10]
(12) Abbreviations: catH, catechol monoanion; cat, catechol dianion; ncatH, 4-nitrocatechol monoanion; Ac, acetyl; H_2 salen, ethylenebis(salicylaldi-

mine).
(13) Raymond, K. N.; Isied, S. S.; Brown, L. D.; Fronczek, F. R.; Nibert, J. H. *J. Am. Chem. Soc.* **1976**, *98*, 1767–1774.
(14) Anderson, B. F.; Buckingham, D. A.; Robertson, G. B.; Webb, J.; Murray, K. S.; Clark, P. E. *Nature (London)* **1976**, *262*, 722–724.
(15) Pfeiffer, P.; Breith, E.; Lübbe, E.; Tsumaki, T. *Justus Liebigs Ann. Chem.* **1933**, *503*, 121.
(16) A description of the physical properties of the Fe(salen) catechol complexes will be reported in a future publication.
(17) Salama, S.; Stong, J. D.; Neilands, J. B.; Spiro, T. G. *Biochemistry* **1978**, *17*, 3781–3785.
(18) National Institutes of Health Predoctoral Trainee, 1978–1979.

Lawrence Que, Jr.,* Robert H. Heistand II[18]
Department of Chemistry, Cornell University
Ithaca, New York 14853
Received November 27, 1978

Iron-Catalyzed Oxidative Decarboxylation of Benzoylformic Acid[1]

Sir:

To identify the chemical roles of iron in biological oxidations and, as well, to develop selective iron oxidants for organic synthesis, we have initiated a mechanistic study of the chemistry of nonporphyrin oxidase enzyme models.[2,3] We herein report a mechanistic characterization of the significant catalysis by soluble iron salts in the oxidative decarboxylation of benzoylformic acid (**1**) to benzoic acid (**2**). This process

$$\underset{\mathbf{1}}{\mathrm{PhC(=O)COH}} + \mathrm{H_2O_2} \xrightarrow{Fe^{2+}} \underset{\mathbf{2}}{\mathrm{PhCO_2H}} + \mathrm{CO_2} + \mathrm{H_2O}$$

mimics, and may thus provide a partial model for, the conversion of α-ketoglutaric acid (αKG) into succinic acid by that class of αKG-dependent mixed-function oxidase enzymes. To the extent that iron in acidic solutions of hydrogen peroxide can produce a manifold of reactive intermediates,[4] our results may have bearing on the role of iron in other Fenton reagent based oxidative processes, such as the Ruff degradation and related decarboxylations.[5]

In aqueous solutions of hydrogen peroxide at pH (H_0) between −1 and +2, **1** undergoes relatively slow decarboxylation to form **2** in essentially quantitative yields.[6,7] The addition of catalytic amounts of ferrous salts (perchlorate, sulfate) to these reaction mixtures causes a dramatic pH-dependent rate enhancement, without reducing the yield of **2.** As listed in Table I, at pH 2.0 ($HClO_4$) the concentration corrected[8] ratio of catalyzed to uncatalyzed reaction rates is 5.6×10^4!

We have previously noted the effects of pH on the kinetics of conversion of **1** into **2** in the absence of iron salts.[6] Hydronium ion and water (spontaneous) catalyzed addition of peroxide to the α-ketocarbonyl of **1** is largely rate limiting in acidic media. The apparent *base*-promoted conversion of **1** into **2** over the pH range −1–2 in the presence of added iron salts (see Table I, k_{cat} increases with increasing pH) clearly demands a new path to product.[9] Likely catalytic roles for iron under our reaction conditions may be to (A) produce hydroxyl radicals, which are responsible for conversion of **1** into **2,** (B) chelate both **1** and an equivalent of hydrogen peroxide to promote decarboxylation through subsequent interactions of these ligands, and (C) undergo oxidation to form a highly oxidized and very reactive iron species prior to the decarboxylation. We conclude that the prior oxidation process is most consistent with the following data.

A radical mechanism propagated by ·OH may be excluded based on experiments in which added EDTA[10] diminishes the rate enhancement induced by iron,[11] since iron–EDTA complexes in aqueous hydrogen peroxide are a recognized source of hydroxyl radicals.[4] Thus, as the EDTA concentration increases from 0 to 4.8×10^{-4} M (at which point the molar ratio of EDTA to iron is unity), k_{obsd} smoothly decreases from 2.8×10^{-2} s^{-1} to 1.5×10^{-3} s^{-1}, the value of k_{obsd} in the absence of added iron (see Table II), and remains invariant with increased concentrations of EDTA. A reasonable interpretation of these data involves simple preferential chelation and sequestering of iron by EDTA, rather than **1.**[12,13] Indeed, the catalytic effect of iron can also be completely deleted by adding fluoride ion which can coordinate and sequester the iron from **1.**[13] Similarly, high concentrations (0.5 M) of phosphate and various carboxylate salts also suppress the rate enhancement due to iron.[13,14]

To differentiate between mechanisms B and C, we have examined (see Table II) the effect of several other metal ions on the kinetics of the oxidative decarboxylation of **1.** Quite likely, many metals would be effective as Lewis acids (for example Al^{3+} or Zn^{2+}), whereas only selected ions could be oxidized to produce metal oxidants that are more reactive than hydrogen peroxide. Iron clearly stands out as a uniquely effective catalyst. Of the other metals studied, only copper and ruthenium exhibit any significant rate enhancement. Most ions have no kinetic effect, and several of the metals (for example, Zn^{2+} and Ag^+) *retard* the conversion of **1** into **2,** most likely through coordinative stabilization of the α-dicarbonyl functionality.[15] Ferric and ferrous salts appear as equally effective catalysts. A critical issue here is identification of the rate-limiting step in the overall conversion of **1** into **2.**[16] One possibility is that interaction of the metal ion with **1** and hydrogen peroxide is slow. This would result from either slow metal ion oxidation or slow ligand substitution. Alternatively, the de-

Table I. Kinetics for Oxidative Decarboxylation of Benzoylformic Acid[a]

pH (H_0)[b]	$10^3 k_0$, M^{-1} s^{-1} [c,e] no iron	k_{cat}, M^{-2} s^{-1} [d,e] iron added	rel rate, enhancement[f] due to iron
−1.0	13	0	0
0.0	7.5	10	1.3×10^3
1.0	4.8	41	8.5×10^3
2.0	2.7	150	5.6×10^4

[a] Reactions were followed spectrophotometrically at 350 nm, at 25 °C. The initial concentration of **1** was 4.8×10^{-3} M. At each pH listed the experimentally determined rate law followed $k_{obsd} = k_0([H_2O_2]) + k_{cat}([H_2O_2][Fe])$ over the given concentration ranges.[c,d] [b] Degassed aqueous $HClO_4$–$NaClO_4$ solutions at 1.0 M ionic strength; see ref 7. [c] Second-order rate constants determined from pseudo-first-order reactions by varying H_2O_2 concentrations between 0.2 and 1.0 M. [d] Third-order rate constants determined at 0.48 M H_2O_2 and catalytic concentrations of $Fe(ClO_4)_2$ of $<5 \times 10^{-4}$ M. [e] Error limits ±10%. [f] Enhancement factor defined by $(k_{cat}/k_0) \times 1$ M; see ref 8.

Table II. Kinetics of Metal Ion Catalyzed Oxidative Decarboxylation of Benzoylformic Acid[a]

metal ion added[b]	$10^3 k_{obsd}$, s^{-1} [c]	metal ion added[b]	$10^3 k_{obsd}$, s^{-1} [c]	metal ion added[b]	$10^3 k_{obsd}$, s^{-1} [c]
none	1.6	Co^{2+}	1.4	Cd^{2+}	1.5
Na^+	1.5	Ni^{2+}	1.6	In^{3+}	1.8
Mg^{2+}	1.2	Cu^{2+}	4.8	Os^{4+}	1.6
Al^{3+}	1.5	Zn^{2+}	0.9	Ir^{3+}	0.9
V^{3+}	1.5	Mo^{6+}	1.9	Pt^{2+}	1.5
Cr^{3+}	1.5	Ru^{3+}	7.6	Au^{3+}	1.0
Mn^{2+}	1.6	Rh^{3+}	1.6	Hg^{2+}	0.7
Fe^{2+}	28.0	Ag^+	0.7	Tl^{1+}	1.3

[a] Temperature 32 °C, pH 2.0, $[H_2O_2] = 0.48$ M, other reaction conditions as described in Table I. [b] Metal ion concentration is 4.8×10^{-4} M. [c] Error limits ±10%.

0002-7863/79/1501-2221$01.00/0